DYNAMIC ANALYSIS OF ARCH DAMS CONSIDERING FLUID-STRUCTURE INTERACTION

ANÁLISIS DINÁMICO DE PRESAS DE ARCO CONSIDERANDO LA INTERACCIÓN FLUIDO-ESTRUCTURA

Yoshi Vela [1]*, Hugo Scaletti [1*,2]

[1]*Facultad de Ingeniería Civil, Universidad Nacional de Ingeniería, Lima, Perú*

[2]*Centro Japón-Perú para la Investigación de Ingeniería Sísmica y Mitigación de Desastres, Lima, Perú*

Received: 05/11/2021 Accepted: 08/08/2022

ABSTRACT

The social, economic, and environmental consequences of the failure of an arch dam make it essential to evaluate its dynamic response to mitigate the risk of a disaster. Since the slenderness and flexibility of these dams tend to increase the fluid-structure interaction during an earthquake, this work compares the dynamic response of a hypothetical arch dam in the Marañón river, in northern Perú, for both full and empty-reservoir conditions. Three formulations were used to estimate the hydrodynamic pressures: Westergaard's added mass, Eulerian and Lagrangian. The comparisons were performed for earthquakes of distinct seismogenic sources, previously matched to a uniform hazard spectrum with a return period of 10000 years. The finite element method was used to derive the seismic demands of the dam-reservoir-foundation system in COMSOL Multiphysics software, carrying out time-history analyses assuming linear elastic behavior of the dam and foundation domains and a massless foundation approach, ignoring the effect of waves propagation in the foundation but considering its stiffness. The results show that the Lagrangian and Eulerian formulations produce similar seismic demands, while Westergaard's added mass formulation is conservative. The full-reservoir condition generally increases the seismic demands, but the results will depend on the boundary conditions assumed for the fluid and the characteristics of the earthquake, among other factors. Earthquakes matched to the same uniform hazard spectrum do not necessarily produce equal dynamic responses.

Keywords: Seismic analysis, Fluid-Structure Interaction, Finite Element Method, Arch dams.

RESUMEN

Las consecuencias sociales, económicas y ambientales de la falla de una presa de arco hacen que sea fundamental evaluar su respuesta dinámica para mitigar el riesgo de un desastre. Dado que la esbeltez y flexibilidad de estas presas tienden a aumentar la interacción fluido-estructura durante un sismo, este trabajo compara la respuesta dinámica de una hipotética presa de arco en el río Marañón, en el norte de Perú, tanto para condiciones de embalse lleno como vacío. Se utilizaron tres formulaciones para estimar las presiones hidrodinámicas: masa añadida de Westergaard, Euleriana y Lagrangiana. Las comparaciones se realizaron para terremotos de distintas fuentes sismogénicas, previamente emparejadas con un espectro de peligrosidad uniforme con un período de retorno de 10000 años. Se utilizó el método de elementos finitos para derivar las demandas sísmicas del sistema presa-reservorio-cimentación en el software COMSOL Multiphysics, realizando análisis de tiempo-historia asumiendo un comportamiento elástico lineal de los dominios de la presa y la cimentación y un enfoque de cimentación sin masa, ignorando el efecto de propagación de ondas en la cimentación pero considerando su rigidez. Los resultados muestran que las formulaciones lagrangianas y eulerianas producen demandas sísmicas similares, mientras que la formulación de masa agregada de Westergaard es conservadora. La condición de reservorio lleno generalmente aumenta las demandas sísmicas, pero los resultados dependerán de las condiciones de contorno asumidas para el fluido y las características del sismo, entre otros factores. Los terremotos que coinciden con el mismo espectro uniforme de amenazas no necesariamente producen respuestas dinámicas iguales.

Palabras Clave: Análisis sísmico, Interacción fluido-estructura, Método de elementos finitos, Presas de arco

1. INTRODUCTION

The fluid-structure interaction is the physical phenomenon that modifies the dynamic response of a structure in contact with a fluid. The slenderness and flexibility of arch dams increase the interaction with the reservoir, this modifies the dynamic characteristics of the dam and; therefore, the dynamic response to earthquakes [1]

Westergaard, in the early 1930s, proposed a pseudo-static formulation to estimate the hydrodynamic pressures in a concrete dam based on certain

* Corresponding author:
yvelac@uni.pe

simplifications [2], further this formulation was known as Westergaard's added mass. Subsequently, this formulation was generalized to include the flexibility and double curvature of arch dams [3], but still with certain limitations. More recent formulations, based on numerical methods, were developed with the advance of computers [4] being the most common the Eulerian [5] and Lagrangian [6] formulations. These formulations try to deal with the simplifications introduced by Westergaard; however, they are not exempt of practical difficulties.

The importance to mitigate the risk of arch dams' failure makes it essential to include criteria not considered in the typical buildings analysis. For this reason, this study compares the dynamic response of a hypothetical arch dam located on the Marañón River considering the fluid-structure interaction under the generalized Westergaard's added mass, Eulerian and Lagrangian formulations, as well as the dynamic response of the empty-reservoir condition. The finite element method, in COMSOL Multiphysics software, is carried out to perform time-history analyses under earthquakes of different seismogenic source: Moquegua (2001, inter-plate), Tarapacá (2005, intra-plate) and Pisco (2007, inter-plate) assuming linear elastic behavior of the dam and foundation domains and a massless foundation approach.

2. BACKGROUND

In the fluid-structure interaction, each physical domain is described by its own differential equations of motion; however, since it is a coupled phenomenon, it is not possible to determine the solution of one domain independently of the other. Therefore, boundary conditions on the common surface, called fluid-structure interface, are required to obtain the coupled solution [7].

The direction, intensity, and frequency content as well as the vertical component of the earthquake and the reservoir boundary conditions are the most relevant factors in the estimation of the hydrodynamic pressure, while the extent of the reservoir is irrelevant for extensions greater than three times the height of the dam [1].

2.1 WESTERGAARD'S ADDED MASS FORMULATION

Westergaard, with certain assumptions, estimated that hydrodynamic pressures are approximate to the inertial effects produced by a prismatic body of water firmly added to the upstream face of the dam and forced to oscillate frictionlessly along with the dam, while the rest of the reservoir remains stationary [2]. These assumptions were: two-dimensional dam of infinite stiffness and vertical upstream face; reservoir of infinite extension in the upstream direction, perfectly incompressible fluid, and small displacements to ignore the effects of surface waves; and ground excitation limited to harmonic oscillation in the upstream-downstream direction with periods greater than 1 second.

Subsequently, this formulation was generalized to include flexibility and double curvature of arch dams, i.e., the direction and magnitude of the hydrodynamic forces vary at each point of the dam [3]. Also, since the added masses increase the mass of the system without modifying its stiffness, the vibration frequencies of the coupled system are lower than the frequencies of the dam alone, which is expected to occur in the fluid-structure interaction phenomenon. However, this generalization is only an extrapolation of the classical Westergaard formulation; therefore, it still ignores the fluid compressibility and the effects of energy dissipation by waves transmission from the reservoir to the dam and the ground, as well as surface waves dissipation [8].

The Generalized Westergaard formulation assumes, like the classical formulation, that the pressure at any point i on the upstream face of the dam is equivalent to consider the inertial effects of a prismatic body of water oscillating with the dam [9] as determined by (1) and shown in Fig. 1:

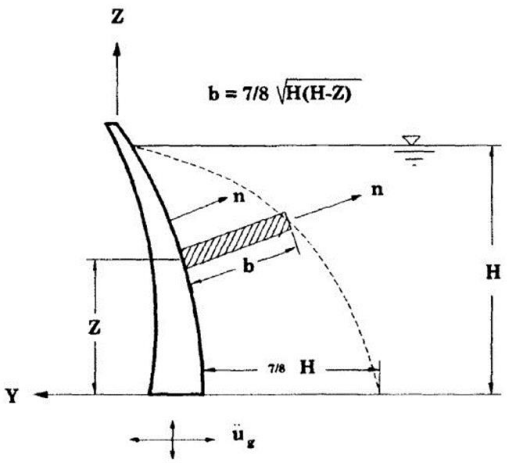

Fig. 1. Westergaard's added mass in arch dams. [9]

$$p_i = b_{(Z_i)}\rho_w \mathbf{n}^T\ddot{\mathbf{u}}_i = \frac{7}{8}\rho_w\sqrt{H(H-Z_i)}\mathbf{n}^T\ddot{\mathbf{u}}_i \quad (1)$$

Under the finite element method interpretation, $\mathbf{n}^T\ddot{\mathbf{u}}_i$ is the normal component of the acceleration at node i, ρ_w the water density, H the depth of the

reservoir, and Z_i the distance from node i to the reservoir bottom. Also, $b_{(Z_i)}$ represents the thickness of the prismatic body of water, of unit length in the X direction, at elevation Z_i.

The vector of equivalent inertial forces at node i ($\mathbf{F}_i$) is obtained by multiplying the pressure and the tributary area ($\mathbf{n}A_i$) of the node i.

$$\mathbf{F}_i = A_i b_{(z_i)} \rho_w \mathbf{n}\mathbf{n}^T \ddot{\mathbf{u}}_i = \mathbf{m}_{a_i} \ddot{\mathbf{u}}_i \qquad (2)$$

Where $\mathbf{m}_{a_i}$ is the matrix of added mass to node i. $\mathbf{F}_i$ is assembled in a similar way to the stiffness matrix; therefore, the matrix of inertial forces ($\mathbf{F}_a$) applied to the dam is:

$$\mathbf{F}_a = \sum \mathbf{F}_i = \mathbf{M}_a \ddot{\mathbf{u}} \qquad (3)$$

$\mathbf{M}_a$ is the matrix of mass to be added in the dam and $\ddot{\mathbf{u}}$ the acceleration vector of the coupled system.

$$(\mathbf{M} + \mathbf{M}_a)\ddot{\mathbf{u}} + \mathbf{C}\dot{\mathbf{u}} + \mathbf{K}\mathbf{u} = \mathbf{0} \qquad (4)$$

$\mathbf{M}$, $\mathbf{C}$, $\mathbf{K}$ are the mass, damping and stiffness matrices for the coupled system, respectively; and $\dot{\mathbf{u}}$, $\mathbf{u}$ are the velocity and displacement vectors for the coupled system, respectively.

2.2 EULERIAN FORMULATION

2.2.1 *Equation of Motion*

The equation of motion of the dam-foundation domain (Ω_s) is described in terms of displacement, while the fluid domain (Ω_f) ones in terms of pressure [10]. Therefore, compatibility and equilibrium at the interface of both systems is ensured by interface equations. COMSOL Multiphysics considers the pressure as degree of freedom defining the fluid domain as an acoustic domain [11].

The equation of motion for the fluid domain or Helmholtz equation (5) is obtained by combining the Navier-Stokes and continuity equations under the Eulerian approach, previously simplified by the following hypothesis: low fluid compressibility, low velocities, and ignore viscous effects as well as body forces [7].

$$\nabla^2 p = \frac{1}{c^2} \ddot{p} \qquad (5)$$

Where ∇ is the gradient operator, p the hydrodynamic pressure and $\ddot{p}$ its second derivative with respect to time, and c the speed of wave sound in water defined in terms of the modulus of compressibility (κ) and the water density as [10]:

$$c = \sqrt{\frac{\kappa}{\rho_w}} \qquad (6)$$

2.2.2 *Boundary Conditions*

The dam-reservoir interface (Γ_I) represents the coupled motion of the dam and the fluid; therefore, the normal displacements at this interface must be compatible in both domains [7]:

$$\mathbf{n}^T \nabla p + \rho_w \mathbf{n}^T \ddot{\mathbf{u}}_s = 0 \qquad (7)$$

Where $\mathbf{n}^T \ddot{\mathbf{u}}_s$ is the normal component of the acceleration in the structure domain.

The reservoir-ground interface (Γ_D) represents the phenomenon of energy dissipation by incidence and reflection of pressure waves on the ground [10]:

$$\mathbf{n}^T \nabla p + \frac{(1-\alpha)}{c(\alpha+1)} \dot{p} = 0 \qquad (8)$$

Where $\dot{p}$ is the first derivative with respect to time of the pressure and α the reflection coefficient defined as the ratio between the amplitude of incident and reflected wave. Typically, it can be considered equal to 0.3 for the sediments deposited on the bottom of the river and equal to 0.7 for the rocks on the lateral slopes.

The free surface (Γ_L) represents the phenomenon of energy dissipation by surface waves. Nevertheless, if the energy dissipation by surface waves is ignored, it can be considered that the hydrodynamic pressure is equal to zero at this surface [7]. This assumption is a valid approximation since the surface waves energy is much smaller than the energy generated by the hydrodynamic pressure.

$$p = 0 \qquad (9)$$

The infinite extension of the reservoir (Γ_T) represents the outcoming waves in the normal direction (no incoming waves) [7], which is known as the equation of Sommerfield.

$$\mathbf{n}^T\nabla p + \frac{1}{c}\dot{p} = 0 \quad (10)$$

Fig. 2 shows the boundary conditions

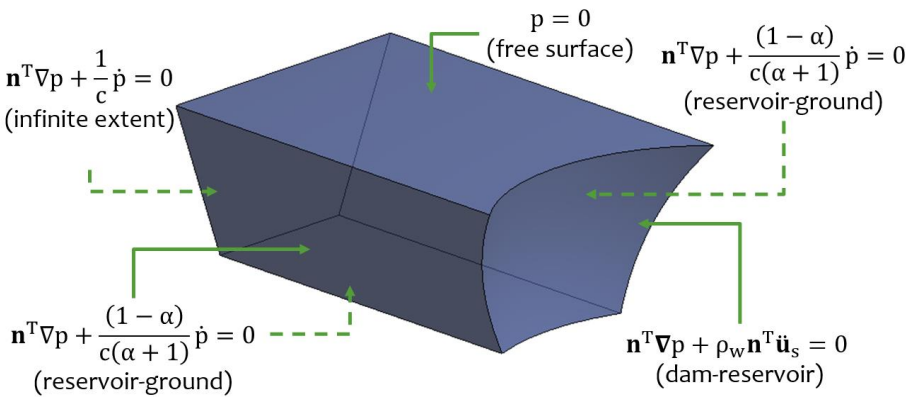

Fig. 2. Boundary conditions – Eulerian formulation

2.2.3 *Discrete Finite Element Formulation*

The discrete form of the equation of motion of dam-foundation domain is obtained by the Galerkin's method and replacing the boundary condition corresponding to the dam-reservoir interface [10].

$$\mathbf{M}_s\hat{\ddot{\mathbf{u}}}_s + \mathbf{C}_s\hat{\dot{\mathbf{u}}}_s + \mathbf{K}_s\hat{\mathbf{u}}_s - \mathbf{R}\,\hat{\mathbf{p}} = \mathbf{F}_s^{ext} \quad (11)$$

Where $\mathbf{M}_s$, $\mathbf{C}_s$, and $\mathbf{K}_s$ are the mass, damping and stiffness matrices respectively for the dam-foundation domain; $\mathbf{R}$ the interaction matrix, and $\mathbf{F}_s^{ext}$ the vector containing the external forces applied to the system. Moreover, $\hat{\ddot{\mathbf{u}}}_s$, $\hat{\dot{\mathbf{u}}}_s$, and $\hat{\mathbf{u}}_s$ are the nodal acceleration, velocity, and displacement vector respectively for the dam-foundation domain and $\hat{\mathbf{p}}$ the nodal pressure vector for the fluid domain.

$$\mathbf{M}_s = \int_{\Omega_S} \mathbf{N}_u^T\rho_s\mathbf{N}_u\,d\Omega \quad (12)$$

$$\mathbf{C}_s = \int_{\Omega_S} \mathbf{N}_u^T\mu_s\mathbf{N}_u\,d\Omega \quad (13)$$

$$\mathbf{K}_s = \int_{\Omega_S} (\mathbf{L}\mathbf{N}_u)^T\mathbf{B}(\mathbf{L}\mathbf{N}_u)\,d\Omega \quad (14)$$

$$\mathbf{R} = \int_{\Gamma_I} \mathbf{N}_u^T\mathbf{n}\mathbf{N}_p\,d\Gamma \quad (15)$$

$$\mathbf{F}_s^{ext} = \int_{\Omega_S} \mathbf{N}_u^T\mathbf{b}_s\,d\Omega \quad (16)$$

$\mathbf{N}_u$ and $\mathbf{N}_p$ are the shape-functions for the displacement and pressure respectively, ρ_s the dam-foundation density, μ_s the dam-foundation viscous damping per unit volume, $\mathbf{L}$ the matrix relating strain and displacements, $\mathbf{B}$ the matrix relating strain and stress, and $\mathbf{b}_s$ the body force in the dam-foundation domain.

The discrete form of the equation of motion for the fluid domain is also obtained by Galerkin's method and replacing the boundary conditions [10].

$$\mathbf{M}_f\ddot{\hat{\mathbf{p}}} + \mathbf{C}_f\dot{\hat{\mathbf{p}}} + \mathbf{K}_f\hat{\mathbf{p}} - \rho_w\mathbf{R}^T\ddot{\hat{\mathbf{u}}}_s = 0 \qquad (17)$$

Where $\mathbf{M}_f$, $\mathbf{C}_f$ and $\mathbf{K}_f$ are the pseudo-mass, pseudo-damping, and pseudo-stiffness matrices respectively for the fluid domain, $\ddot{\hat{\mathbf{p}}}$ and $\dot{\hat{\mathbf{p}}}$ are first and second derivative with respect to time of the nodal pressure vector respectively.

$$\mathbf{M}_f = \frac{1}{c^2}\int_{\Omega_f}\mathbf{N}_p^T\mathbf{N}_p\,d\Omega \qquad (18)$$

$$\mathbf{C}_f = \frac{(1-\alpha)}{c(\alpha+1)}\int_{\Gamma_D}\mathbf{N}_p^T\mathbf{N}_p\,d\Gamma + \frac{1}{c}\int_{\Gamma_T}\mathbf{N}_p^T\mathbf{N}_p\,d\Gamma \qquad (19)$$

$$\mathbf{K}_f = \int_{\Omega_f}\nabla\mathbf{N}_p^T\nabla\mathbf{N}_p\,d\Omega \qquad (20)$$

$\mathbf{R}^T$ allows to transform the hydrodynamic pressures into forces applied on the structure, as well as the accelerations of the structure into hydrodynamic pressures.

These equations can be rewritten in their coupled form as:

$$\begin{bmatrix}\mathbf{M}_s & 0\\ -\rho_w\mathbf{R}^T & \mathbf{M}_f\end{bmatrix}\begin{Bmatrix}\ddot{\hat{\mathbf{u}}}_s\\ \ddot{\hat{\mathbf{p}}}\end{Bmatrix} + \begin{bmatrix}\mathbf{C}_s & 0\\ 0 & \mathbf{C}_f\end{bmatrix}\begin{Bmatrix}\dot{\hat{\mathbf{u}}}_s\\ \dot{\hat{\mathbf{p}}}\end{Bmatrix} + \begin{bmatrix}\mathbf{K}_s & -\mathbf{R}\\ 0 & \mathbf{K}_f\end{bmatrix}\begin{Bmatrix}\hat{\mathbf{u}}_s\\ \hat{\mathbf{p}}\end{Bmatrix} = \begin{Bmatrix}\mathbf{F}_s^{ext}\\ 0\end{Bmatrix} \qquad (21)$$

2.3 LAGRANGIAN FORMULATION

2.3.1 Equation of Motion

The equations of motion of the dam-foundation domain as well as the fluid domain are described in terms of displacement [12]. Moreover, the fluid is assumed to be an elastic and almost incompressible linear material (Poisson's coefficient close to 0.5) without viscosity and irrotational [13].

The hydrodynamic pressure at any point is approximated as the mean stress at that point which is defined, for an isotropic material, as the product of the volumetric strain (ε_f^v) and the modulus of compressibility [7].

$$p = \frac{\sigma_f^x + \sigma_f^y + \sigma_f^z}{3} = -\kappa\varepsilon_f^v \qquad (22)$$

2.3.2 Boundary Conditions

The boundary conditions are like those determined in the Eulerian formulation but expressed in terms of displacements. Fig. 3 shows these boundary conditions.

The dam-reservoir interface (Γ_I) given by:

$$\mathbf{u}_f = \mathbf{u}_s \qquad (23)$$

The reservoir-ground interface (Γ_D) could typically be represented assuming compatibility of displacements between the ground and the reservoir; however, this would ignore the energy dissipation by incidence of waves in the ground. A better alternative is to use viscous dissipators connecting the ground and the reservoir, whose dissipation coefficient for compressional waves is estimated by equivalence between acoustic and mechanical impedance. Since this equivalence is only an approximation, a correlation factor denoted as a is required. In this study a = 0.5 is considered as values between 0.5 and 0.75 seem to be adequate [14].

$$\mathbf{n}^T\boldsymbol{\sigma}_f = a\rho_w c\frac{(1+\alpha)}{(1-\alpha)}\mathbf{n}^T\dot{\mathbf{u}}_f \qquad (24)$$

Where $\boldsymbol{\sigma}_f$ is the tensor stress and $\dot{\mathbf{u}}_f$ the vector velocity in the fluid domain.

The free surface (Γ_L), if it is not considered any constraint on displacements, strains will occur on the surface, which can be interpreted as waves motion.

$$\boldsymbol{\sigma}_f = \mathbf{0} \qquad (25)$$

The infinite extension of the reservoir (Γ_T), Lysmer-Kuhlemeyer viscous dissipators [15] are placed in the direction normal to the surface to dissipate the compressional waves outcoming and reduce the amplitude of the reflected waves on this boundary.

$$\mathbf{n}^T\boldsymbol{\sigma}_f + \sqrt{\kappa\rho_w}\mathbf{n}^T\dot{\mathbf{u}}_f = 0 \qquad (26)$$

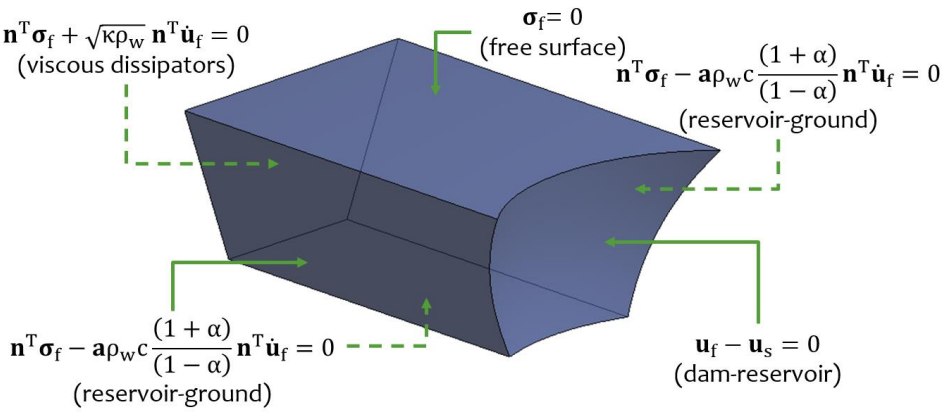

Fig. 3. Boundary conditions – Lagrangian formulation

2.3.3 Discrete Finite Element Formulation

The discrete form of the equation of motion for the dam-foundation domain is like that obtained for the Eulerian formulation except that:

$$\mathbf{R}\,\hat{\mathbf{p}} = \int_{\Gamma_s} \mathbf{N}_{\mathrm{u}}^{\mathrm{T}}\mathbf{t}_{\mathrm{s}}\,\mathrm{d}\Gamma \qquad (27)$$

Where $\mathbf{t}_{\mathrm{s}}$ are the Neumann boundary condition in dam-foundation domain.

A mixed formulation is required to discretize the equation of motion for the fluid domain. The mixed formulation allows expressing the equation in terms of displacement and pressure as independent variables, since, if the equation of motion for the fluid domain is discretized from an irreducible formulation, based on displacements as the only degree of freedom, numerical problems related to volumetric strains may be incurred. These numerical errors occur when considering a high compressibility modulus that fictitiously amplifies the volumetric strains, which in turn generate a fictitious mean stress [7]. COMSOL Multiphysics considers this mixed formulation selecting the option of Nearly Incompressible Material [11].

The discrete form of the equation of motion for the fluid domain is expressed by:

$$\begin{bmatrix}\mathbf{M}_{\mathrm{f}} & 0\\ 0 & 0\end{bmatrix}\begin{Bmatrix}\ddot{\hat{\mathbf{u}}}_{\mathrm{f}}\\ \ddot{\hat{\mathbf{p}}}\end{Bmatrix} + \begin{bmatrix}\mathbf{K}_{\mathrm{f}}^{1} & \mathbf{K}_{\mathrm{f}}^{2}\\ -\mathbf{K}_{\mathrm{f}}^{2^{\mathrm{T}}} & \mathbf{K}_{\mathrm{f}}^{3}\end{bmatrix}\begin{Bmatrix}\hat{\mathbf{u}}_{\mathrm{f}}\\ \hat{\mathbf{p}}\end{Bmatrix} = \begin{Bmatrix}\mathbf{F}_{\mathrm{f}}^{\mathrm{ext}}\\ 0\end{Bmatrix} \qquad (28)$$

Where the matrices $\mathbf{M}_{\mathrm{f}}$, $\mathbf{K}_{\mathrm{f}}^{\mathrm{i}}$, and $\mathbf{F}_{\mathrm{f}}^{\mathrm{ext}}$ are defined by:

$$\mathbf{M}_{\mathrm{f}} = \int_{\Omega_{\mathrm{f}}} \mathbf{N}_{\mathrm{u}}^{\mathrm{T}}\rho_{\mathrm{w}}\mathbf{N}_{\mathrm{u}}\,\mathrm{d}\Omega \qquad (29)$$

$$\mathbf{K}_{\mathrm{f}}^{1} = \int_{\Omega_{\mathrm{f}}} (\mathbf{L}\mathbf{N}_{\mathrm{u}})^{\mathrm{T}}\mathrm{G}\left(\mathbf{D} - \frac{2}{3}\mathbf{m}\mathbf{m}^{\mathrm{T}}\right)\mathbf{L}\mathbf{N}_{\mathrm{u}}\,\mathrm{d}\Omega \qquad (30)$$

$$\mathbf{K}_{\mathrm{f}}^{2} = \int_{\Omega_{\mathrm{f}}} (\mathbf{L}\mathbf{N}_{\mathrm{u}})^{\mathrm{T}}\mathbf{m}\mathbf{N}_{\mathrm{p}}\,\mathrm{d}\Omega \qquad (31)$$

$$\mathbf{K}_{\mathrm{f}}^{3} = \frac{1}{\kappa}\int_{\Omega_{\mathrm{f}}} \mathbf{N}_{\mathrm{p}}^{\mathrm{T}}\mathbf{N}_{\mathrm{p}}\,\mathrm{d}\Omega \qquad (32)$$

$$\mathbf{F}_{\mathrm{f}}^{\mathrm{ext}} = \int_{\Omega_{\mathrm{f}}} \mathbf{N}_{\mathrm{u}}^{\mathrm{T}}\mathbf{b}_{\mathrm{f}}\,\mathrm{d}\Omega + \int_{\Gamma_s} \mathbf{N}_{\mathrm{u}}^{\mathrm{T}}\mathbf{t}_{\mathrm{f}}\,\mathrm{d}\Gamma \qquad (33)$$

Where G is the shear modulus, $\mathbf{D} = \begin{bmatrix}2\mathbf{I}_{3x3} & \mathbf{0}\\ \mathbf{0} & \mathbf{I}_{3x3}\end{bmatrix}$ and $\mathbf{m} = [1,1,1,0,0,0]^{\mathrm{T}}$

These equations can be rewritten in their coupled form as:

$$\begin{bmatrix}\mathbf{M}_{\mathrm{s}} & 0 & 0\\ 0 & \mathbf{M}_{\mathrm{f}} & 0\\ 0 & 0 & 0\end{bmatrix}\begin{Bmatrix}\ddot{\hat{\mathbf{u}}}_{\mathrm{s}}\\ \ddot{\hat{\mathbf{u}}}_{\mathrm{f}}\\ \ddot{\hat{\mathbf{p}}}\end{Bmatrix} + \begin{bmatrix}\mathbf{C}_{\mathrm{s}} & 0 & 0\\ 0 & 0 & 0\\ 0 & 0 & 0\end{bmatrix}\begin{Bmatrix}\dot{\hat{\mathbf{u}}}_{\mathrm{s}}\\ \dot{\hat{\mathbf{u}}}_{\mathrm{f}}\\ \dot{\hat{\mathbf{p}}}\end{Bmatrix} + \begin{bmatrix}\mathbf{K}_{\mathrm{s}} & 0 & 0\\ 0 & \mathbf{K}_{\mathrm{f}}^{1} & \mathbf{K}_{\mathrm{f}}^{2}\\ 0 & -\mathbf{K}_{\mathrm{f}}^{2^{\mathrm{T}}} & \mathbf{K}_{\mathrm{f}}^{3}\end{bmatrix}\begin{Bmatrix}\hat{\mathbf{u}}_{\mathrm{s}}\\ \hat{\mathbf{u}}_{\mathrm{f}}\\ \hat{\mathbf{p}}\end{Bmatrix} = \begin{Bmatrix}\mathbf{F}_{\mathrm{s}}^{\mathrm{ext}}\\ \mathbf{F}_{\mathrm{f}}^{\mathrm{ext}}\\ 0\end{Bmatrix} \qquad (34)$$

3. METHODOLOGY

The dynamic analyses, in the time domain, are carried out with a direct integration method and the generalized alpha algorithm [16], which allows to control the numerical dissipation at high frequencies without introducing considerable dissipation at low frequencies.

Linear and elastic behavior is considered for dam-foundation domain as well as for the fluid domain in the Lagrangian formulation.

3.1 GEOMETRY

The geometry of the dam follows the recommendations of USACE [17]: 175m height, 7.8m width at crest and 33.5m width at base. Moreover, foundation and reservoir extension follow the recommendations of Chopra and Fok [18] as well as the conclusions provided by Sevim et al. [19]: 1900m along the X-axis, 1100m along the Y-axis, and 175m below the dam base level for the foundation, and 555m extension in the upstream direction for the reservoir.

Fig. 4 shows the dimensions of the finite element model.

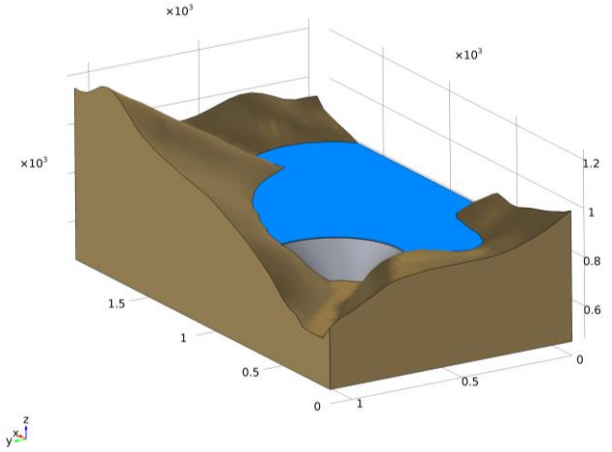

Fig. 4. Dimensions of Finite Element Model in meters – Arch dam

3.2 FINITE ELEMENT MODEL

10-node tetrahedral elements of the Lagrangian family with quadratic shape-functions are used. The Westergaard formulation does not require a fluid domain as the water is represented by added masses per unit area on the upstream face of the dam. On the other hand, the fluid domain is represented as a physical domain in both Eulerian and Lagrangian formulations.

Fig.5 shows the quality of the mesh determined by an absolute scale from 0 to 1 (from low to high quality) [11]. Dam mesh elements are of 15m maximum size and 0.75 average quality, reservoir mesh elements range from 50 to 60m and have 0.67 average quality, and foundation mesh elements range from 50m to 200m and have 0.5 average quality.

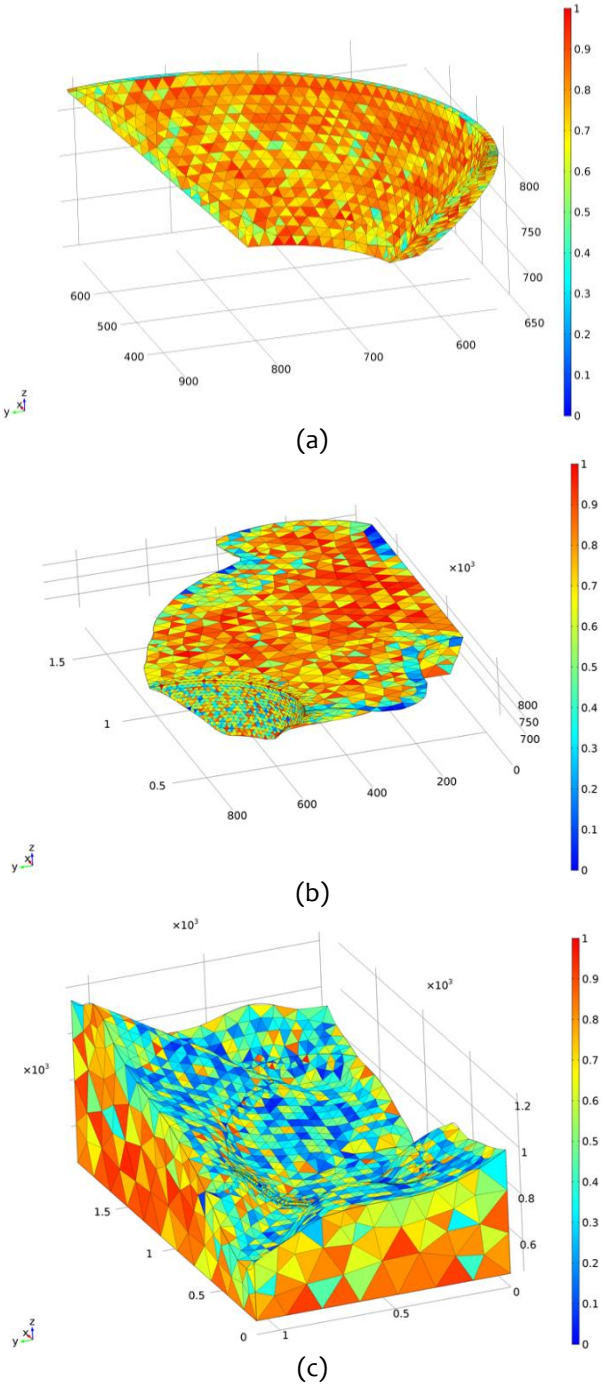

(a)

(b)

(c)

Fig. 5. Quality of the elements (a) Dam, (b) reservoir, and (c) foundation

The mesh sizes used to analyze the model consider the User's guide recommendations of COMSOL Multiphysics for wave propagation problems [20]. When elements of the Lagrangian family with quadratic shape functions are used, these recommendations establish that: First, it is necessary to define a maximum element size equal

to one-fifth of the minimum wavelength to be represented, and then verify if the number of degrees of freedom obtained is at least 1728 times the volume of the model measured in wavelength units.

3.3 MATERIALS

The elastic properties of the concrete dam and the foundation are listed in TABLE I. It is considered 5% Rayleigh damping associated with the first (2.35Hz) and sixth (5.59Hz) vibration modes of the dam-foundation system.

TABLE I. Elastic properties of concrete and foundation

Material	Young's module (MPa)	Poisson	Density (kg/m³)
Concrete	38000	0.25	2300
Foundation (Rock)	65000	0.25	Massless

The elastic (Lagrangian formulation) and acoustic properties (Eulerian formulation) of the reservoir (water) are listed in TABLE II.

TABLE II. Elastic and acoustic properties of water

Formulation	Modulus of Compressibility (MPa)	Poisson	Density (kg/m³)	Wave speed of sound (m/s)	Reflection coefficient	
					Sediments	Rock
Elastic (Lagrangian)	-	-	1000	1440	0.3	0.7
Acoustic (Eulerian)	2100	~0.50	1000	-	0.3	0.7

3.4 DYNAMIC ANALYSIS

The dynamic time-history analyses are performed for synthetic earthquakes determined for the coast of Peru [21], which, following the guidelines of international standards, are previously matched to the uniform hazard spectrum with a return period of 10000 years for the Marañón zone as shown in Fig. 6. Gravity loads are ignored to focus on the dynamic response.

Massless foundation approach is valid to represent the foundation since spatial variations of acceleration along the dam-foundation interface are insignificant in rigid rocks. This approach ignores the effects of waves propagation, but considers the effects of flexibility [22].

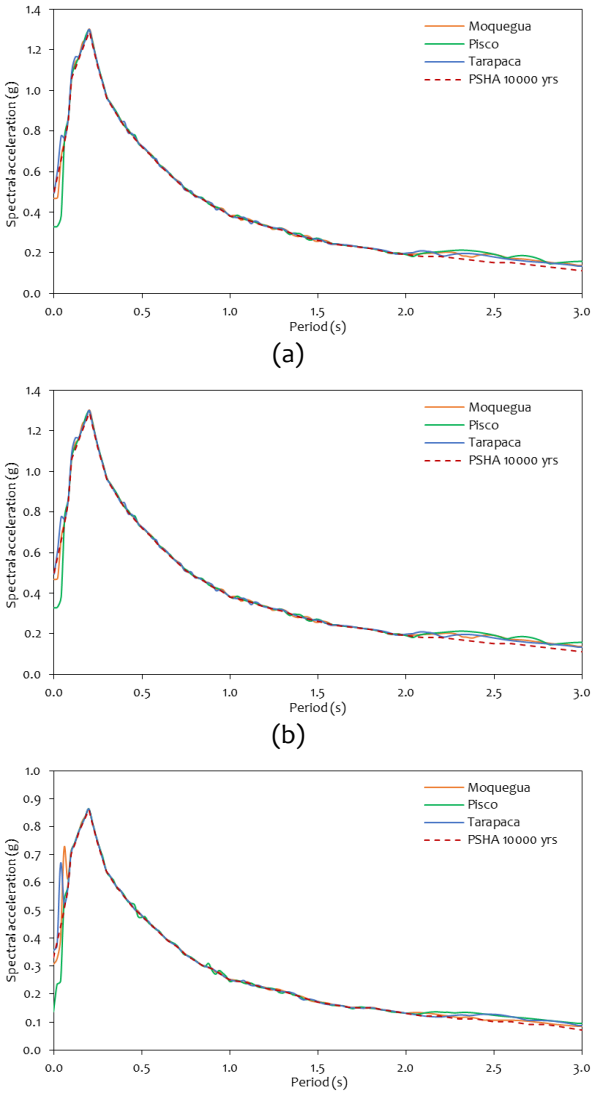

Fig. 6. Spectral acceleration (a) X-direction, (b) Y-direction, and (c) Vertical

4. RESULTS

In the following figures, as a convention, it is considered that the positive displacements and accelerations correspond to movements in the upstream direction.

Fig. 7 shows the maximum relative radial displacements in the central section. Westergaard's formulation produces higher radial displacement than Eulerian and Lagrangian formulations, which produce similar results. Likewise, the empty-reservoir condition produces considerably lower results than the full-reservoir condition, except for the Tarapacá earthquake, which is mainly associated to the frequency content of that earthquake.

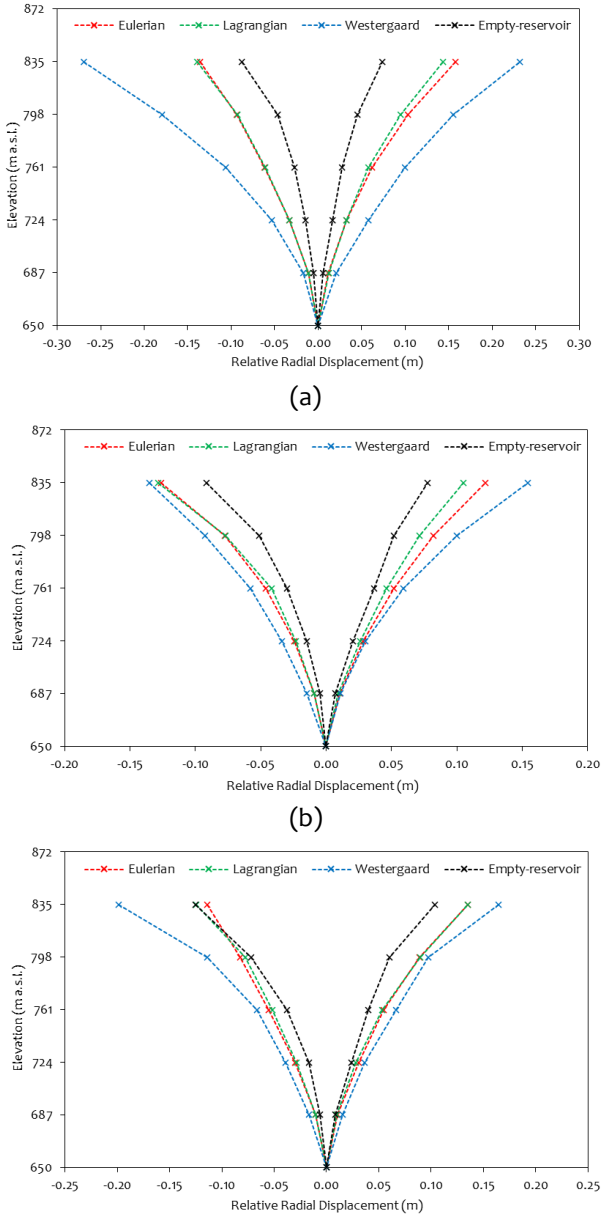

Fig. 7. Relative Radial Displacement at central section (a) Moquegua, (b) Pisco, and (c) Tarapacá

Harmonic analyses are carried out in both horizontal directions to illustrate the dependency of the response with the frequency. Fig. 8 shows that empty-reservoir condition produces higher response than Eulerian formulation for some excitation frequencies.

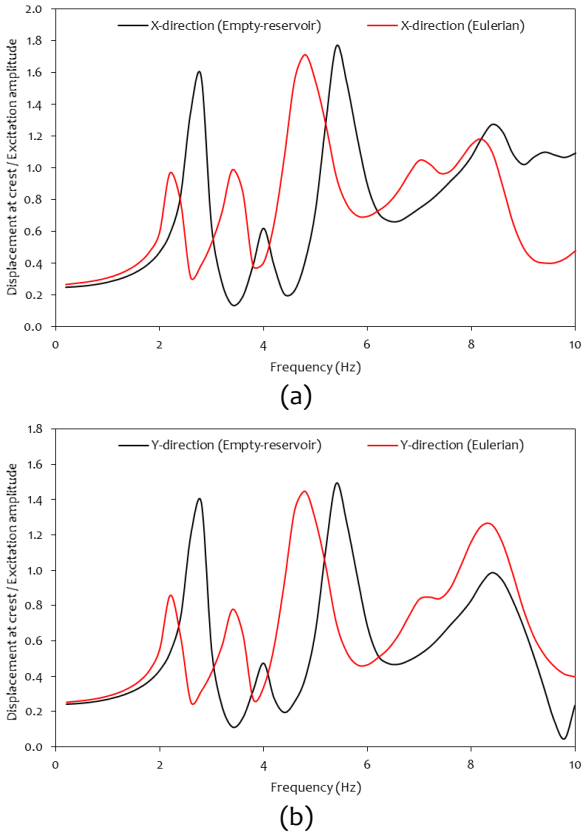

Fig. 8. Radial Displacement at crest / Excitation amplitude (a) X-direction and (b) Y-direction

Fig. 9 and 10 show the time-history of the radial relative displacements and the radial absolute accelerations at the crest, respectively. Eulerian and Lagrangian formulations follow the same response pattern, while Westergaard's formulation and the empty-reservoir condition follow different patterns between them and regarding to the other responses.

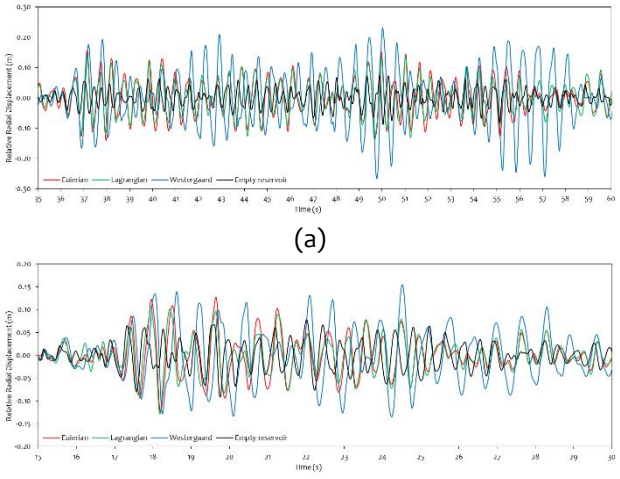

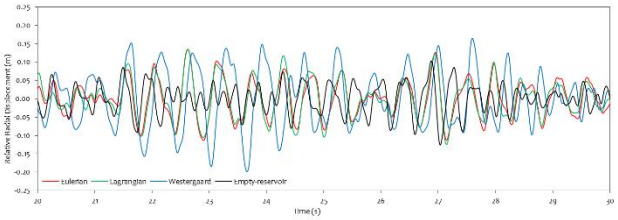

(c)

Fig. 9. Relative Radial Displacement at crest (a) Moquegua, (b) Pisco, and (c) Tarapacá

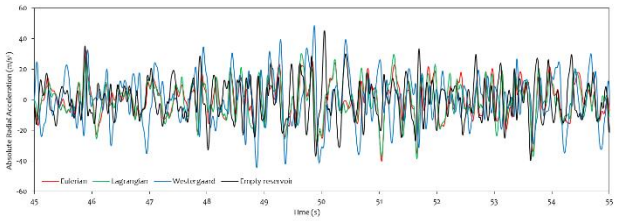

(a)

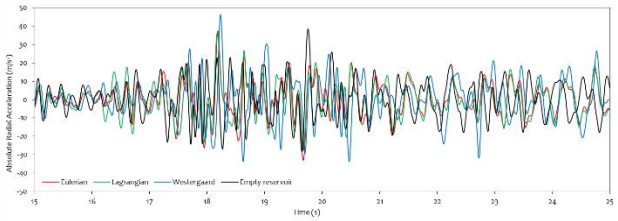

(b)

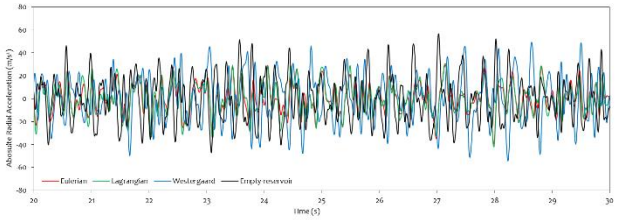

(c)

Fig. 10. Absolute Radial Acceleration at crest (a) Moquegua, (b) Pisco, and (c) Tarapacá

Fig. 11 and 12 show the time-history of hydrodynamic pressures at the bottom of the reservoir (elevation 660 m a.s.l.) and at the mean height of the reservoir (762 m a.s.l.), respectively. Eulerian and Lagrangian formulations follow the same response pattern, from the engineering point of view, while the response for the Westergaard formulation follows a different pattern. Also, hydrodynamic pressure is higher at the mean height than at the bottom of the reservoir as hydrodynamic pressure depends on the acceleration of the dam at each point of the fluid-structure interface in contrast to the hydrostatic pressure that depends only on the depth from the free surface.

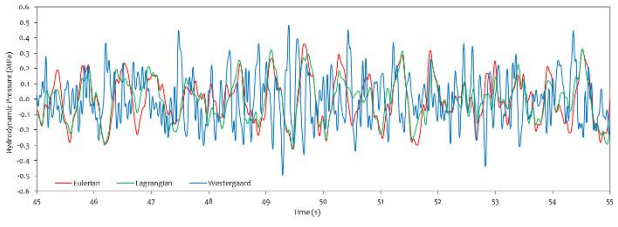

(a)

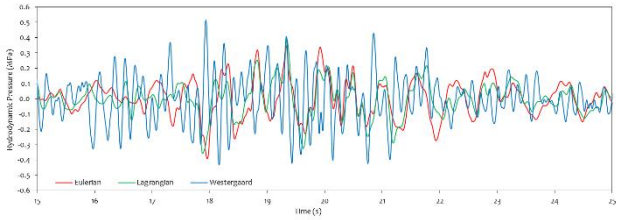

(b)

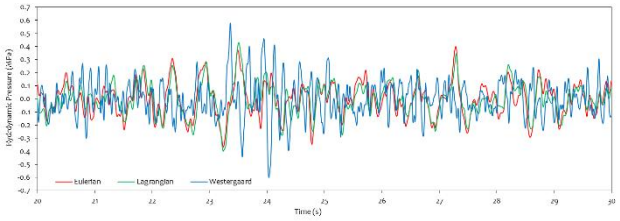

(c)

Fig. 11. Hydrodynamic pressure at bottom of the reservoir (a) Moquegua, (b) Pisco, and (c) Tarapacá

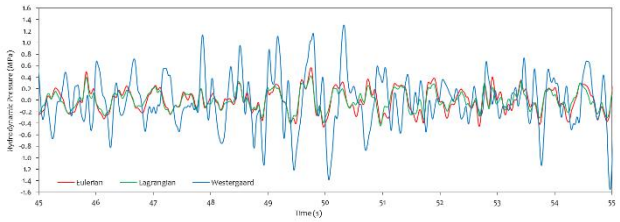

(a)

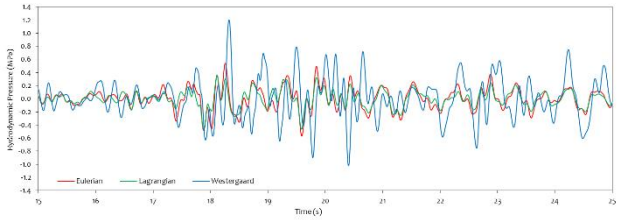

(b)

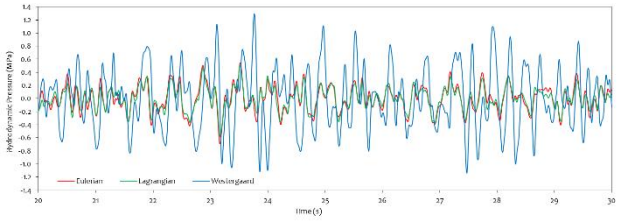

(c)

Fig. 12. Hydrodynamic pressure at mean height of the reservoir (a) Moquegua, (b) Pisco, and (c) Tarapacá

Fig. 13 to 15 show the maximum hydrodynamic pressures. Pressure distribution, maximum values as well as the time when they occur are very similar between the Eulerian and Lagrangian formulations.

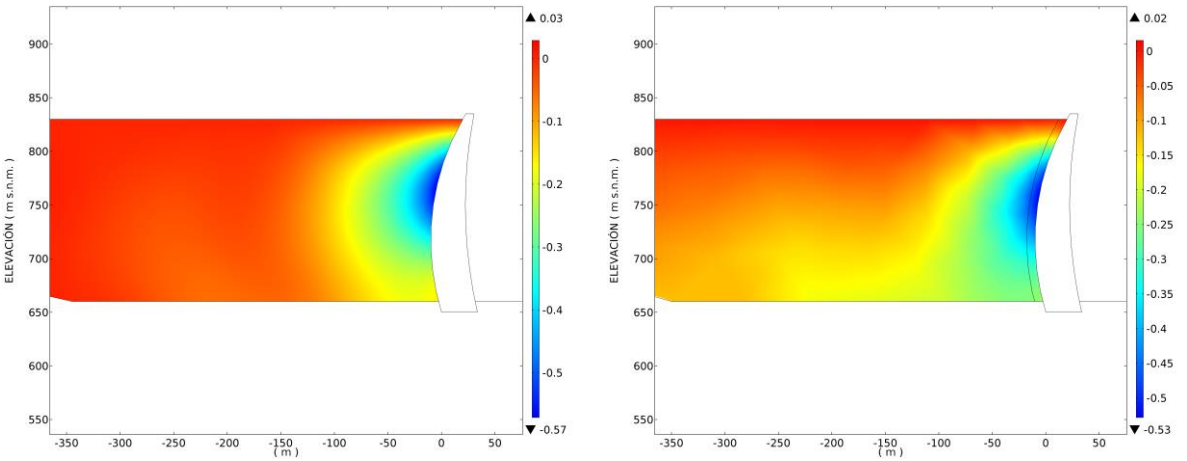

(a) (b)

Fig. 14. Maximum hydrodynamic pressure (MPa) Pisco earthquake (a) Eulerian t=19.59 s and (b) Lagrangian t=19.58 s

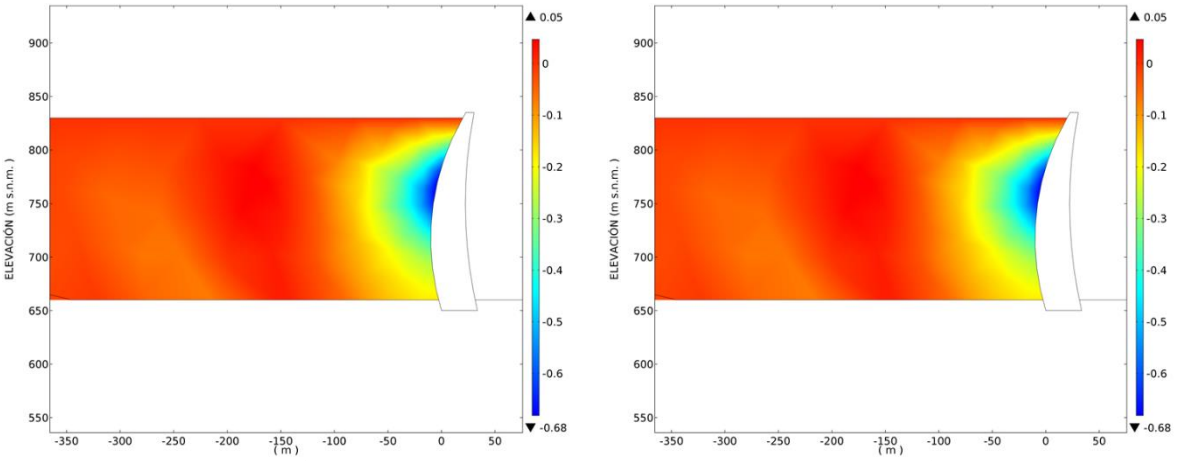

a) b)

Fig. 15. Maximum hydrodynamic pressure (MPa) Tarapacá earthquake (a) Eulerian t=23.16 s and (b) Lagrangian t=23.17 s

Fig. 16 shows the maximum relative radial displacements in the central section. Eulerian and Lagrangian formulations do not show an important variation between the earthquakes. Nevertheless, Westergaard's formulation and the empty-reservoir condition do show higher displacement for Moquegua and Tarapacá earthquakes, respectively.

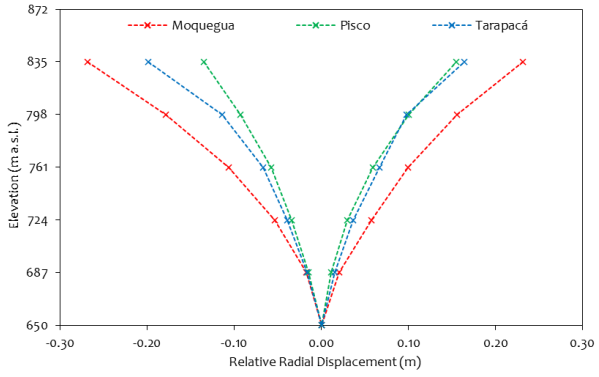

(a)

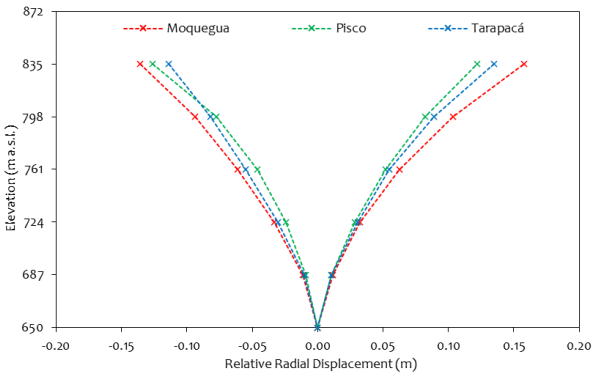

(b)

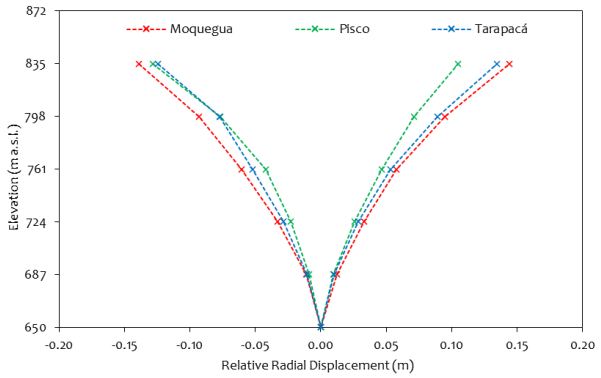

(c)

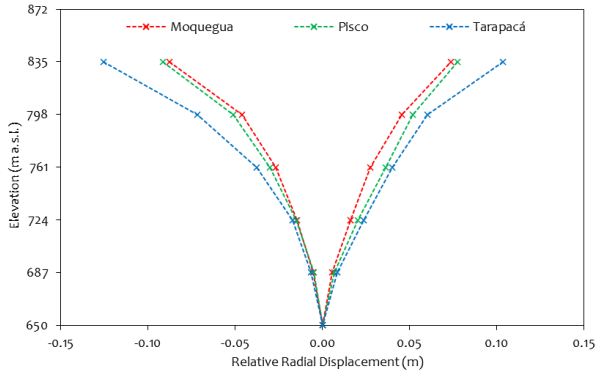

(d)

Fig. 16. Relative Radial Displacement at central section (a) Westergaard, (b) Eulerian, (c) Lagrangian, and (d) Empty-reservoir

CONCLUSIONS

- Westergaard's formulation produces conservative results compared to the other formulations analyzed. Likewise, Eulerian and Lagrangian formulations will produce similar results, from an engineering point of view, if the appropriate parameters are considered for the variables that define the behavior of the model, such as the elastic constants (Poisson's coefficient and compressibility modulus) and boundary conditions, mainly for energy dissipation at the reservoir-ground interface.
- The fluid-structure interaction generally increases the dynamic response of an arch dam with respect to the empty-reservoir condition; however, this will depend on the characteristics of the earthquake considered. As a particular case, in the Moquegua and Pisco earthquakes (inter-plate) a notorious increase of the dynamic response due to the fluid-structure interaction is observed, while in the Tarapacá earthquake (intra-plate) this increase is smaller, even obtaining higher relative radial displacements for the empty-reservoir condition at the elevation near the dam crest respect to Eulerian formulation.
- Lagrangian formulation has the advantage that it can be evaluated in many commercial computer programs.

REFERENCES

[1] J. C. Mosquera, "Efectos hidrodinámicos en el análisis sísmico de presas bóveda," *Ing. Agua*, vol. 2, no. 5, pp. 45–50, Apr. 1995.

[2] H. M. Westergaard, "Water pressure on dams during earthquakes," *Am. Soc. Civ. Eng. Trans.*, no. 1835, pp. 418–433, Nov. 1931.

[3] J. S.-H. Kuo, "Fluid-Structure interactions added mass computations for incompressible fluid," Earthquake Engineering Research Center, University of California, Berkeley, Technical Report N° UCB/EERC-82/09, Aug. 1982.

[4] B. A. Zeidan, "Seismic Finite Element Analysis of Dam-Reservoir-Foundation Interaction," Egypt, 2015, p. 13.

[5] R. Dungar, "An efficient method of Fluid-Structure coupling in the dynamic analysis of structures," *Int. J. Numer. Methods Eng.*, vol. 13, pp. 93–107, 1978.

[6] E. L. Wilson and M. Khalvati, "Finite elements for the dynamic analysis of fluid-solid systems," *Int. J. Numer. Methods Eng.*, vol. 19, pp. 1657–1668, 1983.

[7] O. C. Zienkiewicz and R. L. Taylor, *Finite Element Method: The Basis*, 5th ed., vol. 1. London, 2000.

[8] A. Tahar, "Dynamic Soil-Fluid-Strucutre Interaction Applied for Concrete Dam," Doctoral Thesis, Université Aboubekr Belkaïd Tlemcen, Algeria, 2011.

[9] U. S. Army Corps of Engineers, "Theoretical Manual for Analysis of Arch DamsArch," Department of the Army, Washington, D. C., Technical Report ITL-93-1, Jul. 1993.

[10] F. Sirumbal, "Numerical modeling of dam-reservoir interaction seismic response using the hybrid frequency–time domain (HFTD) method," Master of Science Thesis, Faculty of Civil Engineering and Geosciences, Delft University of Technology, Delft, 2013.

[11] COMSOL, "Reference Manual." 2015.

[12] O. C. Zienkiewicz and P. Bettes, "Fluid - Structure Dynamic Interaction and Wave Forces. An Introduction to Numerical Treatment," *Int. J. Numer. Methods Eng.*, vol. 13, pp. 1–16, 1978.

[13] E. L. Wilson, *Three-dimensional static and dynamic analysis of structures*. Berkeley, California: Computers and Structures, Inc, 2002.

[14] Y. Vela, "Efectos Hidrodinámicos en Presas de Arco," Undergraduate Thesis, Civil Engineering Faculty, National University of Engineering, Lima, Perú, 2018.

[15] J. Lysmer and R. L. Kuhlemeyer, "Finite dynamic model for infinite media," *J. Eng. Mech. Div. - Proc. Am. Soc. Civ. Eng.*, vol. 95, no. 4, pp. 859–877, Aug. 1969.

[16] J. Chung and G. M. Hulbert, "A time Integration Algorithm for Structural Dynamics with Improved Numerical Dissipation: The Generalized-α Method," *ASME J. Appl. Mech.*, pp. 371–375, 1993.

[17] U. S. Army Corps of Engineers, "Arch dam design," Department of the Army, Washington, D. C., Engineer Manual 1110-2–2201, May 1994.
[18] A. K. Chopra and K. L. Fok, "Earthquake analysis and response of concrete arch dams," Earthquake Engineering Research Center, University of California, Berkeley, Technical Report N° UCB/EERC-85/07, Jul. 1985.
[19] B. Sevim, A. C. Altunşşik, A. Bayraktar, M. Akköse, and Y. Calayir, "Water length and height effects on the earthquake behavior of arch dam-reservoir-foundation systems," *KSCE J. Civ. Eng.*, vol. 15, no. 2, pp. 295–303, 2011.
[20] COMSOL, "Acoustic Module - User's Guide" 2015.
[21] Centro Peruano-Japonés de Investigaciones Sísmicas y Mitigación de Desastres CISMID, "Generación de acelerogramas sintéticos para la costa del Perú," Lima, Perú, Technical report commissioned by SENCICO, 2013.
[22] R. W. Clough, K.-T. Chang, H.-Q. Chen, and Y. Ghanaat, "Dynamic interaction effects in arch dams," Earthquake Engineering Research Center, University of California, Berkeley, Technical Report N° UCB/EERC-85/11, Oct. 1985.
[23] Centro Peruano Japones de Investigaciones Sísmicas y Mitigación de Desastres (last accessed on December 2021) Centro de Observación para la Ingeniería Sísmica del CISMID/FIC/UNI [Online]. Available: http://www.cismid.uni.edu.pe/ceois/red/